J. Nonlinear Sci. Vol. 10: pp. 333–354 (2000)
DOI: 10.1007/s003329910013

Journal of
Nonlinear
Science



# Target Patterns and Spirals in Planar Reaction-Diffusion Systems

M. Golubitsky,[1] E. Knobloch,[2] and I. Stewart[3]

[1] Department of Mathematics, University of Houston, Houston, TX 77204-3476, USA

[2] Department of Physics, University of California, Berkeley, CA 94720, USA

[3] Mathematics Institute, University of Warwick, Coventry CV4 7AL, UK

Received February 24, 1999; accepted September 16, 1999
Communicated by Stephen Wiggins

**Summary.** Solutions of reaction-diffusion equations on a circular domain are considered. With Robin boundary conditions, the primary instability may be a Hopf bifurcation with eigenfunctions exhibiting prominent spiral features. These eigenfunctions, defined by Bessel functions of complex argument, peak near the boundary and are called *wall* modes. In contrast, if the boundary conditions are Neumann or Dirichlet, then the eigenfunctions are defined by Bessel functions of real argument, and take the form of *body* modes filling the interior of the domain. Body modes typically do not exhibit pronounced spiral structure. We argue that the wall modes are important for understanding the formation process of spirals, even in extended systems. Specifically, we conjecture that wall modes describe the core of the spiral; the constant-amplitude spiral visible outside the core is the result of strong nonlinearities which enter almost immediately above threshold as a consequence of the exponential radial growth of the wall modes.

## 1. Introduction

Spirals are a universal feature of pattern-forming systems, Murray [26], Cross and Hohenberg [6]. Since their discovery in the celebrated Belousov-Zhabotinsky reaction, spirals have been observed in biological systems, for example in the growth pattern of slime molds (Newell [27]) and in heart muscle (Winfree [38]), in catalysis (Eiswirth et al. [9]), in fluid systems such as convection (Bodenschatz et al. [4]) and the Faraday system (Kiyashko et al. [20]), and even in vibrated sand (Umbanhowar et al. [35]). In some of these cases the spirals form spontaneously; in others a finite amplitude perturbation is necessary to initiate their formation. In some cases the shape of the container, a circular disk for example, is instrumental in facilitating spiral formation; in others spirals form in large aspect ratio systems by a process that is essentially unaffected by the shape of the container. The ubiquity of spirals is in part due to their role as elementary defects in

two dimensions. These defects have topological charge and serve as pacemakers emitting waves that (usually) travel outwards. If multiple defects form from random initial conditions, then the outgoing waves collide, forming a network of shock-like structures separating regions entrained to the local spiral frequency. These regions, each containing a single spiral defect, thus serve as building blocks from which more complex patterns can be constructed.

The formation of spirals (and to a lesser extent target patterns) has been studied from numerous points of view—numerical simulation, matched asymptotic expansions, phase equations, and various phenomenological models. Most easily treated are certain PDE known as $\lambda - \omega$ systems; when truncated at third order in the amplitude, these systems can be written in the form of an (isotropic) complex Ginzburg-Landau equation in the plane. For these PDE Kopell and Howard [21] establish the existence of both target and spiral solutions. Such systems were previously studied by Greenberg [15] who proved the existence of target patterns under more restrictive hypotheses. An important advance was made by Hagan [16] who used perturbation theory to establish, on a formal level, the existence of slowly propagating spiral waves in the complex Ginzburg-Landau equation for eigenvalues with a small imaginary part. Equations of this type describe long wavelength spatial modulation of spatially uniform but temporally oscillating states near onset of oscillation. Although such bifurcations occur in many models of reaction-diffusion systems (Kramer et al. [22]), they may not be present in the physical system itself. Consequently, in the following we take a more general point of view and consider spirals with a finite (as opposed to small) wavenumber in the far field. In this context the most noteworthy recent mathematical contribution is that of Scheel [30], [31], who gives a rigorous proof of the existence of solutions of reaction-diffusion equations in the infinite plane that possess the main characteristics of spirals near infinity. Scheel studies Hopf bifurcation to solutions in the form of appropriately defined (and possibly many-armed) spiral waves, and in particular constructs a finite-dimensional manifold that contains all small rotating waves close to the homogeneous equilibrium. He also relates his results to earlier work on $\lambda - \omega$ systems.

Our aim here is to study the formation of spirals from the viewpoint of symmetric bifurcation theory, treating both spirals and target patterns as general, universal phenomena with many common features. We take as our starting point the natural suggestion that these universal properties of spirals can be understood in terms of a spontaneous symmetry-breaking bifurcation with a nonzero wavenumber, and seek to understand both the nature of this bifurcation and the process by which the resulting instability evolves into a spiral wave in the nonlinear regime.

To do this we find it expeditious to formulate the onset of the instability as a bifurcation problem on a disk, and to examine its properties as the disk radius becomes large. We emphasize that in many of the systems mentioned above a primary bifurcation to spiral waves may not be present in the PDE used to model the system in question. That is, varying model parameters may not create such a bifurcation. For our purposes this is immaterial because such bifurcations can be readily introduced by making changes in the model, for example by introducing additional parameters. Thus such bifurcations are certainly present in the totality of all reaction-diffusion models, and this fact helps us to understand their properties, even in systems where they may arise differently—for example, as the result of a finite-amplitude perturbation.

The paper begins with the observation that with Robin (otherwise called mixed) boundary conditions reaction-diffusion equations on a disk can undergo a Hopf bifurcation from the trivial state, whose associated eigenfunctions have a prominent spiral character. Unlike the Bessel function eigenmodes of DeSimone et al. [8], these eigenfunctions are everywhere smooth; in particular they have no singularity at the center of the disk. They take the form of complex Fourier-Bessel functions, and their amplitude grows rapidly towards the boundary. Consequently we refer to them as *wall* modes. In contrast, with Neumann or Dirichlet boundary conditions, the eigenfunctions take the form of *body* modes filling the interior of the domain but lacking the expected spiral character. For certain parameter values these body modes may, in fact, possess a roughly spiral character, but with "dislocations" at which the strands of the spiral may split or join. If their domain is extended to the infinite plane, the body modes decay to zero at infinity.

The distinction between wall and body modes applies to target patterns as well. Spiral waves in the form of wall modes have previously been found in single reaction-diffusion equations on a disk with "spiral" boundary conditions, Dellnitz et al. [7], and in binary fluid convection in a cylinder with realistic boundary conditions at the sidewall, Mercader et al. [23], but the connection between the mode type (wall or body) and its physical appearance as a spiral has not been emphasized. For example, Scheel shows that the eigenfunctions must take the form of a rotating wave, but his methods do not require an explicit description of their radial structure.

In this paper, we argue that wall modes give insight into why approximately Archimedean spirals are natural in these problems, and that wall modes are important for understanding the formation process of spirals, even in extended systems. In such systems these modes saturate almost immediately above threshold to form the observed extended spiral, with the wall mode being responsible for the structure of the core. In this regime the structure of the resulting spirals is determined by their frequency (which solves a nonlinear eigenvalue problem) and becomes effectively independent of the boundary conditions.

In Section 2 we describe the level curves of complex Fourier-Bessel eigenfunctions and show that these are suitable for describing both spirals and target patterns. In Section 3 we show, using a mixture of analytical and numerical calculations, that solutions of this type are produced naturally as a result of a Hopf bifurcation in systems of reaction-diffusion equations with Robin boundary conditions. We also show that, unlike the situation for Neumann boundary conditions (Auchmuty [2]), there are few restrictions if any on the (azimuthal) mode number of the primary bifurcation, or on the sequence of mode numbers that appear in successive bifurcations from the trivial state.

The paper concludes in Section 4 with a discussion of how the spiral waves obtained here may relate to the spiral waves observed in experiments, and to spirals on the infinite plane.

## 2. Patterns in a Disk

What kinds of pattern should we expect to be generated as solutions of a Euclidean-invariant system of PDE, such as a reaction-diffusion equation, posed on a circular disk?

A partial answer to this question is found by considering solutions that bifurcate from a trivial constant solution. The pattern in these solutions is dominated by the pattern in the eigenfunctions of the associated linearized system of PDE, at least near the primary bifurcation.

### *2.1. Hopf Bifurcation on a Disk*

We consider reaction-diffusion systems whose domain $\Omega$ is a circular disk of radius $R$, defined by

$$U_t = D\Delta U + F(U). \tag{1}$$

Here $U = (U_1, \ldots, U_\ell)^t$ is a $\ell$-vector of functions, $D$ is an $\ell \times \ell$ matrix of diffusion coefficients, and $F$ is an $\ell$-dimensional smooth mapping. The linearized system is

$$U_t = D\Delta U + AU, \tag{2}$$

where $A$, the linearization of $F$ at the origin, is an $\ell \times \ell$ reaction matrix. As we discuss in more detail in Section 3, the eigenfunctions of (2) depend on boundary conditions and are linear combinations of Fourier-Bessel functions. To be specific, let $(r, \theta)$ denote polar coordinates on $\Omega$ and let $J_m$ be the (complex) Bessel function of the first kind of order $m$, for some nonnegative integer $m$. Then a Fourier-Bessel function has the form

$$f(r, \theta, t) = \mathrm{Re}\left[z\, e^{i\omega t + im\theta} J_m(qr)\right], \tag{3}$$

where $q \in \mathbf{C}$ is some nonzero constant and $z \in \mathbf{C}$ is a constant scalar. The possibility that $q$ may be *complex* permits eigenfunctions with spiral geometry.

### *2.2. Patterns*

We assume that the *pattern* associated with a planar function $g$: $\mathbf{R}^2 \to \mathbf{R}$ is given by the level contours of $g$. Typically, the pattern associated with a solution is the pattern of some *observable*, some real-valued function of the (components of the) solution. See Golubitsky et al. [12]. For example, one common observable is the projection onto one component of the solution vector. The observed pattern is then the pattern of a linear combination of $\ell$ Fourier-Bessel functions of the form (3). To gain a feeling for the types of pattern that can form in these systems, we consider the level contours of (3) for some appropriate choices of the resulting eigenfunctions.

We imagine producing patterned solutions via bifurcations obtained through variation of a parameter (typically, a parameter in the reaction matrix $A$). When posed on a disk the primary bifurcation from a spatially uniform equilibrium is either a steady-state bifurcation with $\mathbf{O}(2)$ symmetry or a Hopf bifurcation with $\mathbf{O}(2)$ symmetry. The bifurcation theory of systems with $\mathbf{O}(2)$ symmetry is well developed, and the dynamics associated with the bifurcating solutions is well understood; see Golubitsky et al. [13]. When the critical eigenvalues are simple, the resulting states are $\mathbf{SO}(2)$-invariant, and the patterns of contours consist of concentric circles about the origin. When the critical eigenvalues are double, steady-state bifurcation produces a pitchfork of revolution, and the bifurcating solutions are always invariant under a reflection. In addition, the action of $\mathbf{SO}(2)$ on

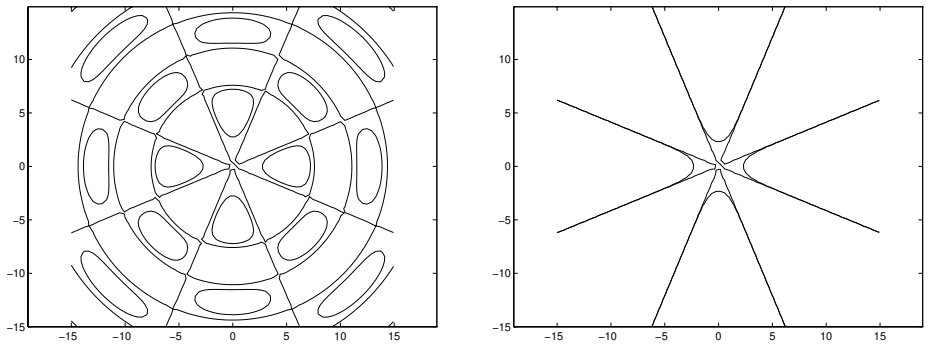


**Fig. 1.** Contour plots of (3) with $m = 4$, $\omega = 0$. (Left) $q = 1$ and (right) $q = i$. Two contours, 0 and 0.1, are shown on a $30 \times 30$ square centered at the origin.

the eigenspace has kernel $\mathbf{Z}_m$ for some integer $m \geq 1$, and the bifurcating solution is then invariant under $m$ different reflections. Hopf bifurcation with double critical eigenvalues produces two distinct symmetry classes of time-periodic states—-a *rotating wave* (time evolution is the same as spatial rotation) and a *standing wave* (which is invariant under a reflection for all time and which undergoes a half-period phase shift when rotated through angle $\pi/m$). In addition, the spatial $\mathbf{Z}_m$ symmetry is present in both solutions.

We now discuss the exact pattern associated with eigenfunctions corresponding to the different $\mathbf{O}(2)$ bifurcations. Which of these eigenfunctions are relevant depends on boundary conditions. In the most familiar cases of Dirichlet boundary conditions ($U = 0$ on $\partial\Omega$) or Neumann boundary conditions ($U_r = 0$ on $\partial\Omega$, where the subscript denotes the partial derivative with respect to $r$), the complex constant $q$ is forced to be real, leading to real-valued Bessel functions $J_m(qr)$ with a real argument. Such eigenfunctions arise, for example, in the vibration of a circular drum; see for example, Courant and Hilbert [5]. On the other hand, as we show in Section 3, Robin (or mixed) boundary conditions ($(U_j)_r + \beta_j U_j = 0$ on $\partial\Omega$) can lead to eigenfunctions with complex $q$. Then $J_m(qr)$ becomes a complex-valued function on the line $\{qr\colon\ r \in \mathbf{R}\}$ in the complex plane. Complex $q$ have also been observed when using spiral boundary conditions ($U_r = K U_\theta$ on $\partial\Omega$), see Dellnitz et al. [7], and in oscillatory convection with realistic lateral boundary conditions, Mercader et al. [23].

After scaling, we may assume $|q| = 1$. The patterns associated with $q = \pm 1$ are well known. When $m \geq 1$, the time-independent states have patterns with $m$ radial nodal lines and a number of concentric nodal circles (Figure 1(left)). The position of the nodal circles relative to the boundary depends on the details of the boundary conditions. The amplitude of the eigenfunction decays like $r^{-1/2}$, so all contours except the zero contour are bounded. In the corresponding Hopf bifurcation, the instantaneous time contours are as in Figure 1(left); in the rotating wave the contours rotate at a uniform speed about the origin, and in the standing wave the nodal lines are fixed while the remaining contours oscillate up and down periodically. Note that one cannot distinguish between these two possibilities because the snapshot retains an $m$-fold reflection symmetry. However, if the pattern of Figure 1(left) represents a rotating wave, we expect this symmetry to be broken once nonlinear terms are added.

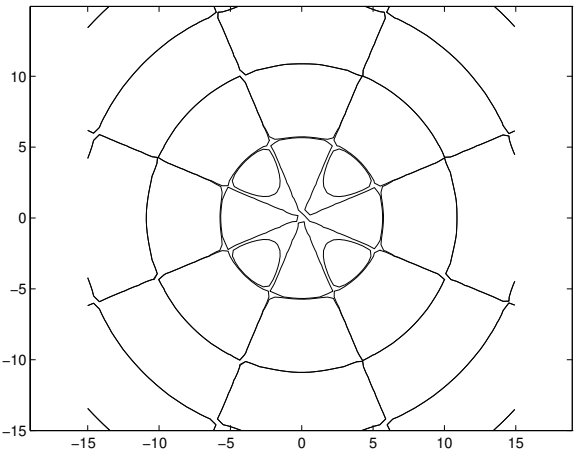


**Fig. 2.** Contour plot of (4) with $m = 4$, $q = e^{i\pi/4}$. Two contours, 0 and 0.1, are shown on a $30 \times 30$ square centered at the origin.

Another exceptional case arises when $q = \pm i$. Now there are just $m$ radial nodal lines (Figure 1(right)). Solutions of this type cannot occur with either Neumann or Dirichlet boundary conditions. This is because one of the two independent eigenfunctions is $K_m(|q|r)$ which is singular at $r = 0$ and must therefore be discarded while the other, $I_m(|q|r)$, has no (real) zeros. However, with identical Robin boundary conditions on all species, solutions of this type are possible although there is at most one, cf. Friedlander and Siegmann [10]. This is in contrast to the case of real $q$, for which there is a countable number of solutions.

In general, however, $q$ is complex ($q \neq \pm 1, \pm i$) and the structure of the possible eigenfunctions does not appear to be widely known. Presumably this is because the traditional boundary conditions employed in many problems are either Dirichlet or Neumann. For $q$ that is neither real nor imaginary, and $m > 0$, the functions $J_m(qr)$ are neither real nor purely imaginary. As already discussed, in steady-state bifurcation theory the nonlinear theory picks an eigenfunction that is invariant under a reflection—say reflection across the real axis. Such a function has the form

$$\mathrm{Re}\left[\left(e^{im\theta} + e^{-im\theta}\right) J_m(qr)\right]. \tag{4}$$

The level contours of (4) are shown in Figure 2.

The contours of the rotating wave in the corresponding Hopf bifurcation are the contours of (3) at an instant of time—an $m$-armed spiral (Figure 3). In time, these contours rotate rigidly with uniform angular velocity, Mercader et al. [23]. The amplitude of these complex Bessel functions $J_m(qr)$ grows exponentially with $r$ instead of decreasing algebraically, as in the case of $q$ real. The standard asymptotic formula for Bessel functions, discussed in Section 2.3, shows that the spiral is asymptotically Archimedean (spaced equally in the radial direction) for large $r$. In practice this approximately equal spacing also remains valid for quite small $r$.

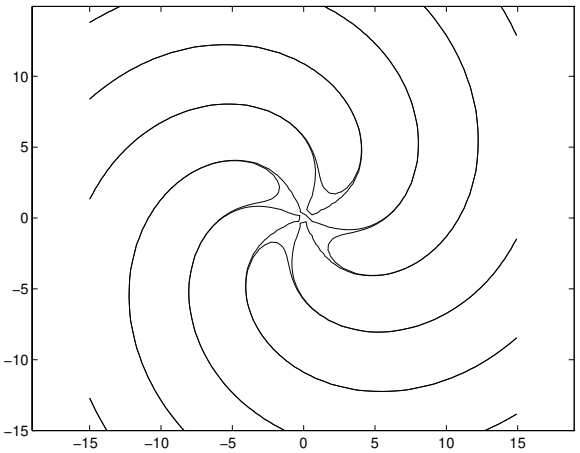


**Fig. 3.** Contour plot of (3) with $m = 4, q = e^{i\pi/4}, t = 0$. Two contours, 0 and 0.1, are shown on a $30 \times 30$ square centered at the origin.

The standing wave in this Hopf bifurcation has nodal lines as in Figure 2, and the nonzero contours oscillate periodically in time. However, the phasing of this oscillation is such that the circular sections of the contours drift outward from the origin in a wave-like motion, cf. [23]. When $m = 0$ the eigenfunction (3) has no $\theta$-dependence, and the level contours are concentric circles about the origin, as expected. Figure 4 shows a time sequence of the level contours showing these contours propagating radially as in a *target pattern*. Again the amplitude of the eigenfunction grows exponentially in $r$.

### *2.3. Asymptotics of Bessel Functions*

We now briefly describe how to employ the standard asymptotic expansion of Bessel functions, Whittaker and Watson [36], to verify the above statements analytically. Recall that we are dealing with eigenfunctions of the form

$$f(z, \theta, t) = \mathrm{Re}[e^{i\omega t + im\theta} J_m(z)],$$

where $z = re^{i\psi}$. For large $|z|$ the asymptotics of Bessel functions imply that

$$f(z, \theta, t) \sim \sqrt{\frac{1}{2\pi r}} e^{r \sin\psi} \cos\left(\omega t + m\theta - \frac{\psi}{2} - r\cos\psi + \frac{m\pi}{2} + \frac{\pi}{4}\right), \quad \sin\psi > 0, \tag{5}$$

$$f(z, \theta, t) \sim \sqrt{\frac{1}{2\pi r}} e^{r|\sin\psi|} \cos\left(\omega t + m\theta - \frac{\psi}{2} + r\cos\psi - \frac{m\pi}{2} + \frac{\pi}{4}\right), \quad \sin\psi < 0. \tag{6}$$

The zero-sets of the asymptotic eigenfunctions are easily determined. For simplicity we assume $\sin\psi > 0$. The case $\sin\psi < 0$ is similar, with a few minor changes. The

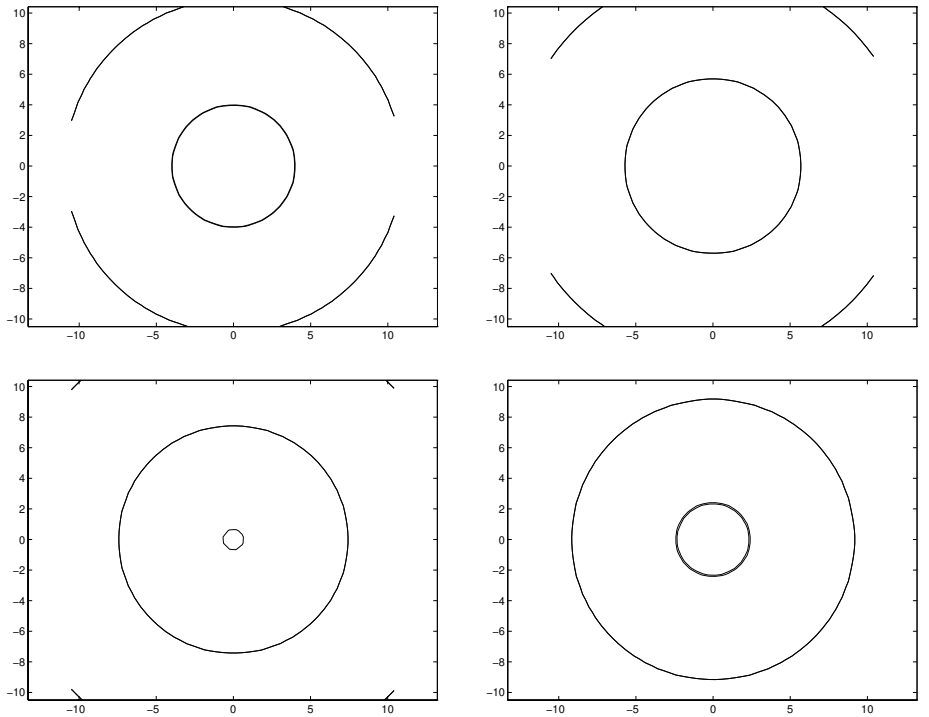

**Fig. 4.** Contour plot of (3) with $m = 0$, $q = e^{0.35i\pi}$, $\omega = 1$, $t = 0, \frac{\pi}{4}, \frac{\pi}{2}, \frac{3\pi}{4}$. Two contours—0, 0.1—are shown on a $20 \times 20$ square centered at the origin.

zero set of (5) comprises those points $(r, \theta)$ in polar coordinates for which

$$\omega t + m\theta - \frac{\psi}{2} - r\cos\psi + \frac{m\pi}{2} + \frac{\pi}{4} = (2s+1)\frac{\pi}{2}, \tag{7}$$

for integer $s$. It is easy to see that when $m > 0$ and $\psi \neq (2k+1)\frac{\pi}{2}$ for integer $k$, this zero-set is a rotating $m$-armed set of Archimedean spiral pairs whose "pitch" $p = \frac{2m\pi}{\cos\psi}$. By "Archimedean spiral pair," we mean that the zero-set is comprised of $m$ curves, each consisting of two separate Archimedean spirals which interlace with each other and meet at the origin (see Fig. 3); each member of this pair moves radially by a distance $p$ as the spiral makes one full turn round the origin. The structure of double spirals is natural because we are considering the zero contour, and we expect to find spiral regions in which the function is positive, separated from spiral regions in which it is negative.

However, when $\psi = (2k+1)\frac{\pi}{2}$, the function $J_m(e^{i\psi})$ is either real or purely imaginary, depending on $m$. In this case for even $m$ (5) is replaced by

$$f(z,\theta,t) \sim \sqrt{\frac{1}{2\pi r}}e^r \cos(\omega t + m\theta)\cos\left((m-k)\frac{\pi}{2}\right), \qquad \sin\psi > 0, \tag{8}$$

with a similar expression involving $\sin(\omega t + m\theta)$ for odd $m$. Thus at given $t$ the only nodes are at $\theta = (2s+1)\frac{\pi}{2m} - \frac{\omega t}{m}$ and there is no outward (or inward) propagation.

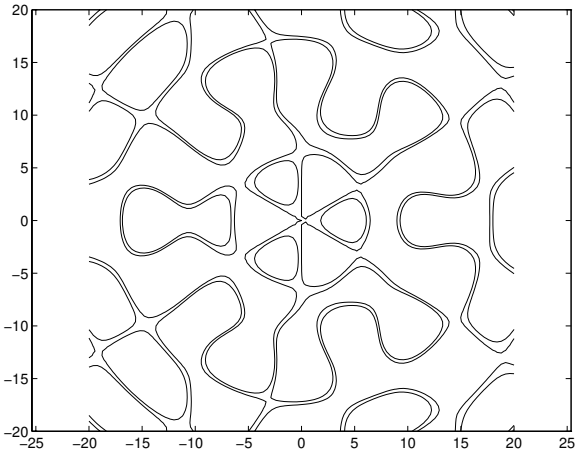


**Fig. 5.** Contour plot of $\cos(3\theta)J_3(r) + 2.5\cos(8\theta)J_8(0.7r)$. Two contours, 0 and 0.1, are shown on a $40 \times 40$ square centered at the origin. Courtesy of V.G. LeBlanc.

The case $m = 0$ is exceptional. Here we get target patterns with no fixed nodal lines, provided again $\psi \neq (2k+1)\frac{\pi}{2}$.

### *2.4. Mode Interactions*

The eigenfunctions (3) can also produce a number of other unexpected patterns, even in the case $q$ real. A striking instance arises in the work of Palacios et al. [29] on models of the flame experiments of Gorman et al. [14] on cellular flames. Here a "mode interaction," leading to a superposition of Bessel functions of different orders, generates concentric rings consisting of different numbers of cells—for example, a ring of three cells surrounded by a ring of seven cells. In the interior the pattern appears to have $\mathbf{D}_3$ symmetry, and near the boundary the pattern appears to have $\mathbf{D}_7$ symmetry (Fig. 5). In fact, it has neither. The observation of Palacios et al. [29] sheds light on the puzzling "almost symmetries" of the experimental states; the observation itself depends upon the fact that the supports of the two Bessel functions are almost disjoint.

We conclude that the geometry of planar patterns generated by Bessel functions is much richer than normally assumed. Indeed we have only begun to explore and understand the possibilities. It is also noteworthy that, apart from the exponential growth of amplitude, the spirals and target patterns in Figures 3 and 4 closely resemble states observed in reaction-diffusion systems, in particular the celebrated BZ reaction, Winfree [37], Müller et al. [25]. We have not found this remark in the extensive literature on such patterns; possibly solutions of this type have been rejected because of their exponential growth. (Spiral-contoured eigenfunctions involving Bessel functions $Y_n(z)$ of the second kind as well as those of the first kind have long been known—see DeSimone et al. [8]—but because of the occurrence of $Y_n(z)$, these eigenfunctions are singular at the origin.)

### *2.5. Relation to Nonlinear Waves*

We suggest that exponential growth is no reason for discarding eigenfunctions of the form (3). On the contrary, such eigenfunctions have a number of important attributes, in addition to the above, which indicate that they may well provide a new way to understand the mathematics of targets and spiral waves. In particular we believe that the exponential growth is not an obstacle because in the nonlinear PDE the amplitude of the waves must saturate almost immediately above threshold, thereby generating spiral waves of approximately uniform amplitude outside of a core region, as observed in experiments (see Section 4). Moreover, the exponential growth favors the spiral appearance of the modes. The reason is that for a mode with complex amplitude $f_m(r)$, we have

$$\mathrm{Re}[f_m(r)e^{i\omega t+im\theta}] = |f_m(r)|e^{i\omega t+im\theta+i\Phi_m(r)}.$$

For an exponentially growing mode, $\Phi_m(r)$ is likely to be *monotonic*. It is this property that produces a well-defined spiral, and that typically fails for body modes.

In the next section we show that in reaction-diffusion systems on a disk, with Robin boundary conditions, there can and do exist Hopf bifurcations to spirals (and targets) corresponding to eigenfunctions of the form (3).

## 3. Reaction-Diffusion Equations

### *3.1. General Case*

We study the primary bifurcation in the system (2), written in the form

$$U_t = D\Delta U + (B + \sigma I)U, \tag{9}$$

using the method of Goldstein et al. [11]. Here $\sigma \in \mathbf{R}$ is the bifurcation parameter, $U = U(r, \theta, t)$, and the linear problem (9) is to be solved subject to Robin boundary conditions (RBC)

$$(U_j)_r + \beta_j U_j = 0 \quad \text{on} \quad r = R. \tag{10}$$

In the following we assume that the $\beta_j$ are all distinct; this assumption excludes the case of Neumann or Dirichlet boundary conditions on $U$. We look for Hopf bifurcations and make the *ansatz* that

$$U(r, \theta, t) = e^{i\omega t}V(r, \theta).$$

Substituting this assumption into (9) yields the eigenvalue problem

$$D\Delta V + (B + \lambda I)V = 0, \tag{11}$$

where $\lambda = \sigma - i\omega$. To solve this problem we assume that $V$ is an eigenfunction of the Laplacian,

$$\Delta V = -k^2 V.$$

Then (11) reduces to

$$(B + \lambda I - k^2 D)V = 0, \tag{12}$$

so that (nontrivial) solutions exist provided

$$\det(B + \lambda I - k^2 D) = 0. \tag{13}$$

Equation (13) is a polynomial of degree $\ell$ in $k^2$. Thus there are $\ell$ roots $k_1^2, \ldots, k_\ell^2$, assumed to be distinct, which are functions of the complex quantity $\lambda$. Let $V_j \equiv (v_j^1, \ldots, v_j^\ell)$ be the nullvector of (12) corresponding to $k_j^2$.

We now choose a fixed value of $m$. Using separation of variables we can write the solutions to (11) as

$$V(r, \theta) = \mathrm{Re}\left[a_1 J_m(k_1 r) e^{im\theta} V_1 + \cdots + a_\ell J_m(k_\ell r) e^{im\theta} V_\ell\right],$$

where $a_1, \ldots, a_\ell$ are complex constants. Applying Robin boundary conditions to $V$ on the disk of radius $R$ for all $t$ implies that the real parts of the $\ell$ expressions

$$\begin{gathered}\left\{a_1 v_1^1 (k_1 J_m'(k_1 R) + \beta_1 J_m(k_1 R)) + \cdots + a_\ell v_\ell^1 (k_\ell J_m'(k_\ell R) + \beta_1 J_m(k_\ell R))\right\} e^{i(\omega t + m\theta)}, \\ \vdots \\ \left\{a_1 v_1^\ell (k_1 J_m'(k_1 R) + \beta_\ell J_m(k_1 R)) + \cdots + a_\ell v_\ell^\ell (k_\ell J_m'(k_\ell R) + \beta_\ell J_m(k_\ell R))\right\} e^{i(\omega t + m\theta)},\end{gathered}$$

vanish. These equations hold for all $\theta$ precisely when

$$\begin{aligned} a_1 v_1^1 (k_1 J_m'(k_1 R) + \beta_1 J_m(k_1 R)) + \cdots + a_\ell v_\ell^1 (k_\ell J_m'(k_\ell R) + \beta_1 J_m(k_\ell R)) &= 0, \\ &\vdots \\ a_1 v_1^\ell (k_1 J_m'(k_1 R) + \beta_\ell J_m(k_1 R)) + \cdots + a_\ell v_\ell^\ell (k_\ell J_m'(k_\ell R) + \beta_\ell J_m(k_\ell R)) &= 0. \end{aligned}$$

There is a nontrivial solution to these complex equations for $a_1, \ldots, a_\ell$ precisely when

$$\det \begin{pmatrix} v_1^1 (k_1 J_m'(k_1 R) + \beta_1 J_m(k_1 R)) & \cdots & v_\ell^1 (k_\ell J_m'(k_\ell R) + \beta_1 J_m(k_\ell R)) \\ \vdots & & \vdots \\ v_1^\ell (k_1 J_m'(k_1 R) + \beta_\ell J_m(k_1 R)) & \cdots & v_\ell^\ell (k_\ell J_m'(k_\ell R) + \beta_\ell J_m(k_\ell R)) \end{pmatrix} = 0. \tag{14}$$

Note that when the $\beta_j$ are distinct we expect the $k_j$ to be distinct also.

### *3.2. Systems of Two Equations*

When $\ell = 1$ it is easy to show that all bifurcations are steady-state and the corresponding eigenfunctions are body modes. This is no longer the case when $\ell \geq 2$. In the following we examine the case $\ell = 2$ and write

$$B = \begin{pmatrix} a & b \\ c & d \end{pmatrix}.$$

In this case $bc < 0$ is a necessary condition for the presence of a Hopf bifurcation; if $bc > 0$ all bifurcations are necessarily steady regardless of the values of $\beta_1$, $\beta_2$. To find explicit Hopf bifurcations with eigenfunctions in the form of wall modes, we define

$$z_1 = k_1 R \quad \text{and} \quad z_2 = k_2 R,$$

and

$$\widetilde{\beta}_1 = \beta_1 R \quad \text{and} \quad \widetilde{\beta}_2 = \beta_2 R,$$

and write equation (14) in the form

$$\begin{array}{lcl} v_1^1 v_2^2 (J_m'(z_1)z_1 + \widetilde{\beta}_1 J_m(z_1))(J_m'(z_2)z_2 + \widetilde{\beta}_2 J_m(z_2)) & - & \\ v_2^1 v_1^2 (J_m'(z_2)z_2 + \widetilde{\beta}_1 J_m(z_2))(J_m'(z_1)z_1 + \widetilde{\beta}_2 J_m(z_1)) & = & 0. \end{array} \tag{15}$$

In general this is a complex equation for $\sigma$ and $\omega$. Bessel functions satisfy the identity

$$zJ_m'(z) = zJ_{m-1}(z) - mJ_m(z).$$

This identity is useful even when $m = 0$ because $J_{-1} = -J_1$. Then (15) implies that

$$\begin{array}{lcl} v_1^1 v_2^2 (J_{m-1}(z_1)z_1 + (\widetilde{\beta}_1 - m)J_m(z_1))(J_{m-1}(z_2)z_2 + (\widetilde{\beta}_2 - m)J_m(z_2)) & - & \\ v_2^1 v_1^2 (J_{m-1}(z_2)z_2 + (\widetilde{\beta}_1 - m)J_m(z_2))(J_{m-1}(z_1)z_1 + (\widetilde{\beta}_2 - m)J_m(z_1)) & = & 0. \end{array} \tag{16}$$

### *3.3. Numerical Results in Two Dimensions*

In this section we describe the solution of equation (16) for a particular choice of the matrices $D$ and $B$ and the coefficients $\beta_1$, $\beta_2$. We solve this equation numerically using Matlab. First we used a graphical method to locate parameter values at which the primary bifurcation is to a nonzero mode number, and then we used Matlab's PDE toolbox to solve the linearized equation (11) numerically and compute eigenfunctions. The two methods yield results in close agreement.

To locate suitable parameter values we sketched—for the range of mode numbers $0 \le m \le 5$—the curves along which the real and imaginary parts of the left-hand side of (16) vanish, as $\sigma$ and $\omega$ vary within suitable ranges. We experimented with parameter values until the first bifurcation was to a nonzero mode number. This occurs, for example, at parameter values

$$D = \begin{pmatrix} 0.01 & 0 \\ 0 & 0.015 \end{pmatrix} \quad \text{and} \quad B = \begin{pmatrix} 0.5 & 1 \\ -1 & 0 \end{pmatrix},$$

with

$$R = 1, \quad \beta_1 = 10, \quad \text{and} \quad \beta_2 = 0.01;$$

see Figure 6.

In this example the mode numbers of the primary bifurcations occur in the order 3, 1, 4, 2, 5, 0, as $\sigma$ increases. By definition, the eigenfunctions corresponding to nonzero mode numbers have the symmetry of a rotating wave but lack reflectional symmetry. In our terminology they are therefore "spiral," although as already discussed they are "good spirals" only when they are in addition wall modes. Despite the appearance of some of the figures, this is in fact so for all the $m \neq 0$ eigenfunctions illustrated, even for $m = 3$, 1, and 4. Thus in this example the primary bifurcation is to a 3-armed ($m = 3$) spiral, while the bifurcation to a target pattern ($m = 0$) occurs only much later. This behavior is very different from what happens with Neumann boundary conditions (and positive definite $D$) for which the first instability is always $m = 0$.

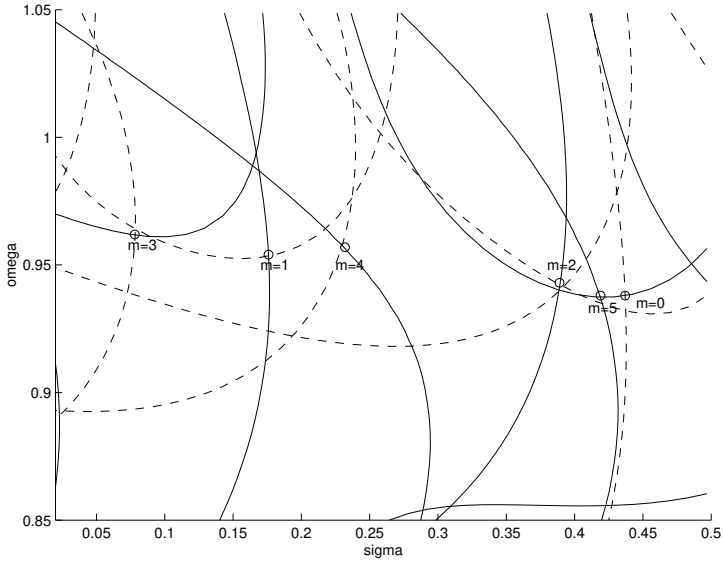


**Fig. 6.** Solutions to (16) when $m = 0, \ldots, 5$ given by intersections of the zeros of the real (solid curves) and imaginary parts (dashed curves) of (16). Open circles indicate intersection points and are labelled by mode number.

Solutions of the PDE (11) for these parameter values using the PDE toolbox confirm the eigenvalues and mode numbers obtained with greater accuracy from (16) and shown in Figure 6. Repeated refinements of the mesh were used to check convergence of the PDE calculation. Table 1 lists the resulting values of $\lambda$, $\omega$ and the associated values of $m$. Figures 7–12 show the corresponding eigenfunctions in the form of both contour plots and three-dimensional plots. The experiment by Hartmann et al. [17] on the NO + CO reaction on a small circular Pt(100) catalyst shows a spiral whose Karhunen-Loève decomposition reveals the presence of $m = 1, 2, 3$ modes with structure remarkably like that shown in these plots. Such states are also found in the Barkley model of excitable media [17]. Note that despite its appearance as a rotating "pulse," the $m = 1$ mode is part of the family of spirals. Moreover, as argued below, we believe that for infinite domains the eigenfunctions illustrated here correspond to the *core* of a spiral wave, and note that the spiral geometry observed in simulations and experiments is far more evident to the eye outside the core than it is within it.

**Table 1.** Numerical data for the first six eigenmodes obtained from the PDE.

| Real Part $\sigma$ | Imaginary Part $\omega$ | Mode Number $m$ |
|---|---|---|
| 0.080 | 0.961 | 3 |
| 0.179 | 0.953 | 1 |
| 0.234 | 0.957 | 4 |
| 0.396 | 0.941 | 2 |
| 0.415 | 0.951 | 5 |
| 0.445 | 0.937 | 0 |

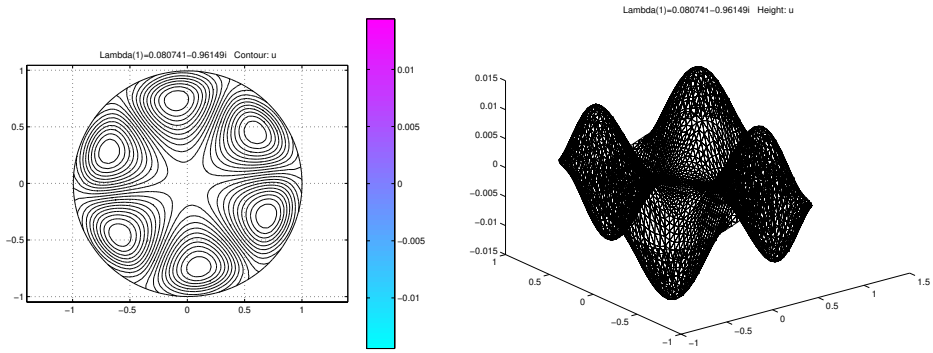


**Fig. 7.** Contours and three-dimensional plot of numerically computed eigenfunctions for (16) at first eigenvalue, for which $m = 3$.

Since $\omega \neq 0$ the roots $k^2$ of (13) are necessarily complex and the eigenfunctions take the form of wall modes. Note that the requirement $\omega \neq 0$ is not necessary: It is possible for $k^2$ to be complex even when $\omega = 0$ since the quadratic equation for $k^2$ may not have real roots. However, the point is that for Robin boundary conditions with $\beta_1 \neq \beta_2$ this is inevitable, and in this sense model-independent. When $\beta_1 = \beta_2 \equiv \beta$ (this case includes both Neumann and Dirichlet boundary conditions), the solution takes the form of a *single* Bessel function with $k^2$ real. There is a countable number of solutions with $k^2 > 0$ (body modes) and (if $\beta \neq 0, \infty$) at most one solution with $k^2 < 0$ (a wall mode), cf. Friedlander and Siegmann [10].

## 4. Relation to Observed Spirals

Center manifold reduction can now be used to establish the presence of nonlinear spirals (rotating waves) and target patterns (standing waves), as in the familiar analysis of the Hopf bifurcation with $\mathbf{O}(2)$ symmetry, Golubitsky et al. [13]. As we have seen, when $q$

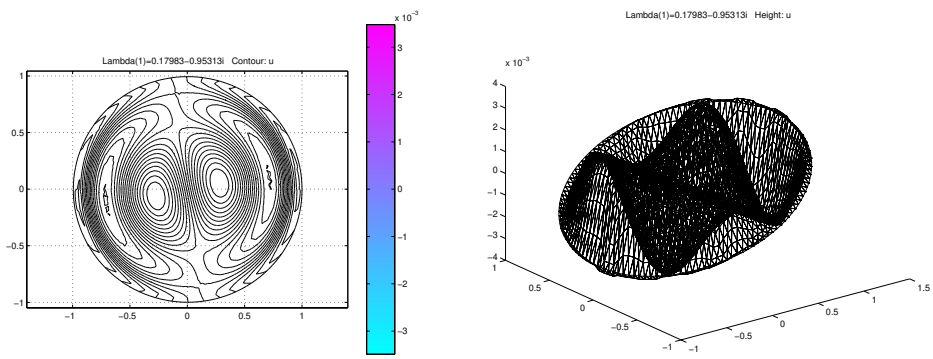


**Fig. 8.** Contours and three-dimensional plot of numerically computed eigenfunctions for (16) at second eigenvalue, for which $m = 1$.

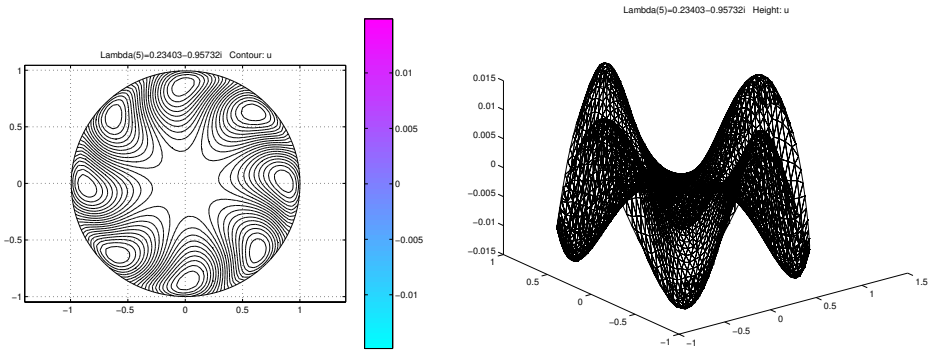


**Fig. 9.** Contours and three-dimensional plot of numerically computed eigenfunctions for (16) at third eigenvalue, for which $m = 4$.

is neither real nor purely imaginary, the spirals consist of waves that travel outwards and at the same time rotate azimuthally. The targets are an equal-amplitude superposition of clockwise and counterclockwise rotating $m$-armed spirals and so have $m$-fold reflection symmetry; as a result they do not rotate, although the waves do continue to propagate radially outwards.

Solutions to nonlinear equations, obtained via bifurcation analysis, resemble appropriate linear eigenfunctions. This is because local bifurcation theorems guarantee only solutions with sufficiently small amplitude. However, when the linear eigenfunction involves a complex Bessel function, the amplitude of the eigenfunction increases exponentially from the center to the boundary, forcing the domain of validity of the (weakly) nonlinear theory to be much smaller than might otherwise be expected. This increase of amplitude also leads to interpretational difficulties in physical space, since exponentially growing spiral states do not resemble the spirals of approximately uniform amplitude that are observed in chemical or fluid systems.

Nevertheless, there may be a simple and completely natural relation between the exponentially growing states predicted by a local bifurcation analysis, and the finite-

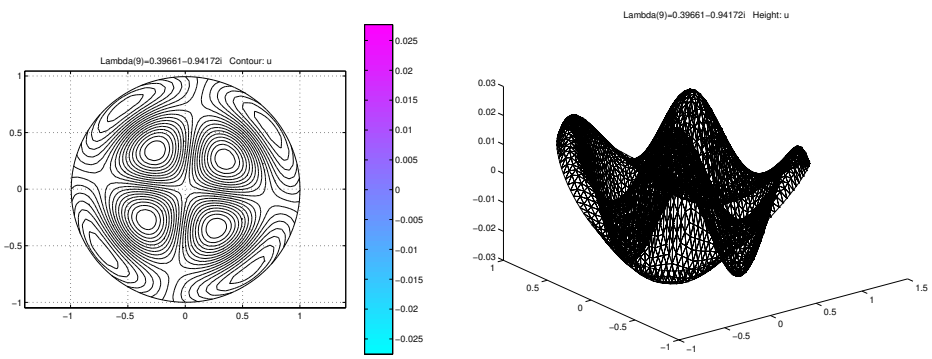


**Fig. 10.** Contours and three-dimensional plot of numerically computed eigenfunctions for (16) at fourth eigenvalue, for which $m = 2$.

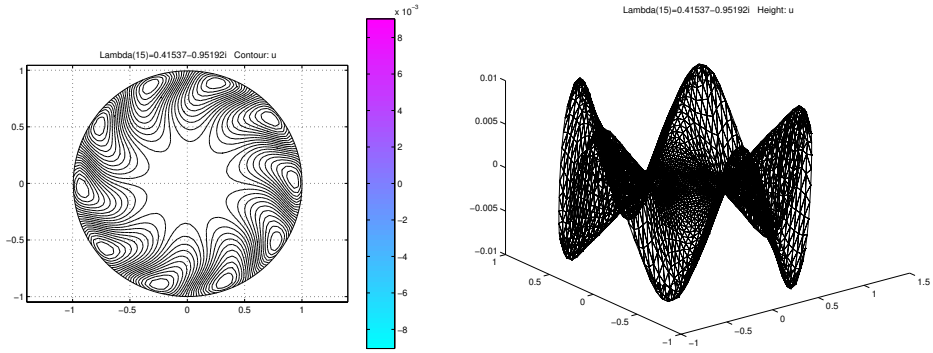


**Fig. 11.** Contours and three-dimensional plot of numerically computed eigenfunctions for (16) at fifth eigenvalue, for which $m = 5$.

amplitude spiral states observed in experiments. At the moment this relation is speculative, but there is substantial supporting evidence. This presumed relationship follows from distinctions between *convective* and *absolute* instabilities on the unbounded plane, as we now explain.

### *4.1. Convective and Absolute Instabilities*

Both target and spiral patterns have a prefered direction of propagation, i.e., the waves travel *either* outward *or* inward. This preference for one direction is a consequence of the circular geometry (it is not present when the problem is posed on a line) and is important because it introduces the distinction between convective and absolute instability into the problem. These concepts have been developed to describe the evolution of localized perturbations in unbounded domains. In a convective instability the perturbation grows only in a reference frame moving with the group velocity; at any given location the disturbance eventually *decays*. In contrast when the instability is absolute the perturbation grows at *all* locations.

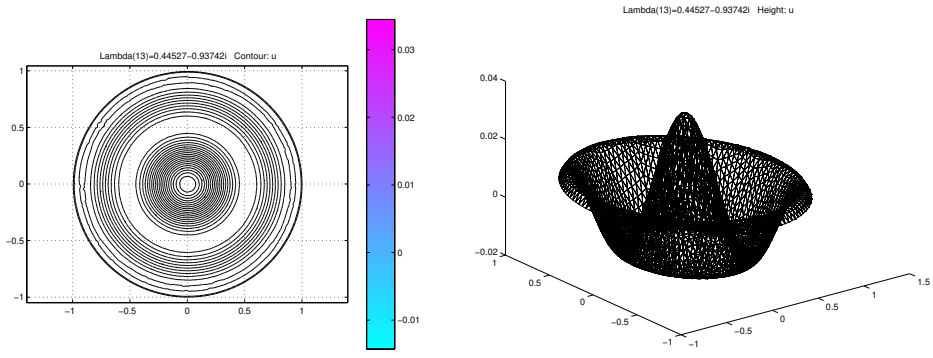


**Fig. 12.** Contours of numerically computed eigenfunctions for (16) at sixth eigenvalue, for which $m = 0$.

The consequences of these ideas are most easily described for systems defined on an interval $0 < x < L$, but with a preferred direction of propagation introduced by adding an advection term as in Tobias et al. [34]. In the following we suppose that the group velocity is to the right and discuss first the unbounded system on a line. In such a system, let $\sigma_c$ be the value of the bifurcation parameter $\sigma$ at which the trivial state first becomes unstable. Near $\sigma_c$ the resulting instability is convective because its growth rate is necessarily small compared to the (finite) advection rate. Also, let $\sigma_a > \sigma_c$ be the value of $\sigma$ at which the instability of the trivial state in the unbounded system first becomes absolute—that is, the point at which instabilities begin to grow at *every* location; see Bers [3], Huerre and Monkewitz [18]. Of course, this distinction is meaningful only when considering the initial value problem for localized disturbances. For our purposes the important point about absolute instability is that its onset is associated with the presence of a double root of the (complex) dispersion relation for infinitesimal waves in the complex wavenumber plane, subject to a certain "pinching" condition, Bers [3], Huerre and Monkewitz [18]. The double root condition, together with the dispersion relation, suffices to determine $\sigma_a$ and the associated *complex* wavenumber $k_a$ and *real* frequency $\omega_a$. In general $\operatorname{Im} k_a \neq 0$. Consequently at $\sigma = \sigma_a$ a wave propagating away from $x = 0$ amplifies *spatially* with an *exponential* growth rate $\operatorname{Im} k_a$. In a finite domain, the convective instability manifests itself as a transient growth of a perturbation that ultimately decays unless $\sigma$ exceeds a higher threshold $\sigma_f$ at which an unstable eigenmode first appears. The important point is that in large domains, $\sigma_f = \sigma_a + \mathcal{O}(L^{-2})$ and $\omega_f = \omega_a + \mathcal{O}(L^{-2})$, and that the eigenfunction inherits the exponential growth from the unbounded system, Tobias et al. [34].

Numerical calculations of target patterns on a disk resulting from Hopf bifurcation, Tobias and Knobloch [33], suggest that these ideas carry over to target patterns, and more generally to spirals as well. This is plausible since in local patches both spirals and target patterns are very close to traveling waves whose cross-section in the direction of propagation is close to the one-dimensional case, with a slow variation in the transverse direction related to the curvature of the wavefront. The relation between the classical linear stability calculation and the onset of absolute instability makes it clear why in general the linear eigenfunctions in large domains grow exponentially with $r$, and therefore why eigenfunctions of this type are the proper eigenfunctions to use even on an unbounded domain. Moreover, the observation that $\sigma_f \to \sigma_a$ as $R \to \infty$, where $\sigma_f$ is the Hopf bifurcation point determined in Section 3, implies that in an unbounded system such exponentially growing "eigenfunctions" are present from the onset at $\sigma = \sigma_a$.

### *4.2. Nonlinear Theory*

So far this is all linear theory. In the nonlinear regime Tobias et al. [34] distinguish three regimes. In the first, the weakly nonlinear theory alluded to above applies; for the problem on the interval $0 \leq x \leq L$ Tobias et al. [34] find that this happens only within an $\mathcal{O}(L^{-5})$ neighborhood of $\sigma_f$. Thus only very close to the primary absolute instability will the solutions resemble the linear eigenfunctions *globally*. For somewhat larger values of the bifurcation parameter ($\sigma - \sigma_f = \mathcal{O}(L^{-2})$) the growing wave develops into a (usually) stationary *front* at some $x = x_{front} < L$. This front is a fully nonlinear state of the system and connects $\mathcal{O}(1)$ amplitudes at $x_{front} < x < L$ to exponentially small

amplitudes near $x = 0$. When the front is stationary and *no phase slips* occur at the front, the frequency $\omega_f$ is conserved across the front, and thus selects both the amplitude and the (real) wavenumber of the (saturated) waves in the postfront region ($x > x_{front}$). Thus in this regime the frequency $\omega_f$ selected near $x = 0$ by *linear* theory determines all the properties of the outward-moving *fully nonlinear* waves in $x > x_{front}$. With further increase in $\sigma$ the location of the front moves towards $x = 0$ until, when $\sigma - \sigma_f = \mathcal{O}(1)$, the linear regime near $x = 0$ is eliminated. At this point the boundary at $x = 0$ no longer selects the frequency $\omega_f$; instead the selected frequency $\omega$ must be found as a solution to a nonlinear eigenvalue problem. Tobias et al. [34] find that in this regime the dependence of $\omega$ on the parameter $\sigma$ becomes more noticeable, but that it continues to be essentially independent of the boundary conditions. Thus the wavenumber and amplitude of the wave in the postfront regime continue to be selected in the core, with only a thin boundary layer present near $x = L$, in which the solution adjusts to the imposed boundary conditions.

This picture is well established for unidirectional waves on a line. Recent simulations by Tobias and Knobloch [33] indicate that analogous regimes are present for target patterns in the complex Ginzburg-Landau and FitzHugh-Nagumo equations. Almost immediately above threshold the nonlinear solution begins to depart from the eigenfunction. This occurs first near the boundary where the amplitude of the wall mode is largest, and leads to the creation of a front separating the core region from an essentially constant amplitude but fully nonlinear wave outside of the core. With increasing $\sigma$ the core of the target narrows as the front moves gradually inwards; when $\sigma$ is large enough the selected frequency starts to differ from that predicted by the linear theory. At this point the structure of even the core begins to depart from the form of the linear eigenfunction. At the same time the amplitude of the waves outside the core region continues to increase and so does the selected wavenumber—that is, the wavelength of the pattern decreases, Tobias and Knobloch [33]. Of course it may happen that the selected waves in the postfront region are themselves unstable (convectively or absolutely), as discussed by Aranson et al. [1] and Tobias and Knobloch [33] (see also Bär and Or-Guil [28]), but the basic picture, of a nonlinear front separating a core region from fully nonlinear (outward) traveling waves outside the core, remains. As before, we expect solutions of this type to be essentially independent of the (outer) boundary conditions. The boundary conditions may therefore be homotopically continued to Neumann or Dirichlet boundary conditions and very similar solutions will be found—at least for large enough $\sigma$. That is, nonlinear solutions of the observed form should be present even in systems in which there may be *no* primary Hopf bifurcation to a wall mode.

These suggestions are fully consistent with the work of Hartmann et al. [17] who compute nonlinear spiral solutions to the Barkley model of excitable media with Neumann boundary conditions on a circle of radius $R$ and corroborated experimentally. Decreasing $R$ leads to an increase in frequency prior to the disappearance of stable spirals at a saddle-node bifurcation, i.e., extinction. Thus no Hopf bifurcation to stable spirals occurs in this model. The observed increase in the spiral frequency as $R$ decreases is attributed to the resulting compression of the core; in the calculations of Tobias et al. [34] a similar compression occurs with increasing $\mu$ and is also associated with an increased frequency, as calculated from the nonlinear eigenvalue problem. Other models of excitable media exhibit similar behavior, Zykov and Müller [39].

The view of spirals that emerges suggests that in large domains the region in parameter space where linear or weakly nonlinear theory provides a global description of target or spiral patterns is very small—in fact, so small as to be practically undetectable. In a somewhat larger parameter range (though still small) the eigenfunctions (wall modes) of the linear theory describe only the inner part of the core, while the visible part of these patterns, separated from the core by a front, is fully nonlinear and hence inaccessible to local bifurcation theory. For general values of the bifurcation parameter, $\sigma - \sigma_f \gg R^{-2}$, no part of these patterns resembles the solutions generated by linear theory. In no case, however, is the core of these patterns a singularity—indeed solutions of elliptic PDE in a disk are everywhere regular, Courant and Hilbert [5]. All singular eigenfunctions must be discarded and play no role in the core structure, Dellnitz et al. [7].

The resulting picture of a spiral suggests a reinterpretation of the spiral boundary condition introduced by Dellnitz et al. [7] as an *effective* boundary condition that may be applied at the location of the front separating the core from the visible spiral in order to study the core region of the spiral. In this view the condition is not a *boundary* condition but a *matching* or *transition* condition between the core and the fully nonlinear regime. This boundary condition forces the presence of a spiral. However, more generally, nonlinear spiral solutions to reaction-diffusion systems may be constructed by matching a solution valid near $r = 0$ to one valid as $r \to \infty$, as demonstrated by Hagan [16] and Scheel [30]. At the requisite matching radius we expect nonzero radial fluxes of the concentration, suggesting that the Robin boundary conditions employed here may also be viewed as effective boundary conditions to be applied at the core-spiral boundary in unbounded domains, with our approach providing a description of the solution in the core. In fact, Robin boundary conditions may apply even in finite systems in the presence of chemically active boundaries, Hartmann et al. [17]. In our approach these boundary conditions provide a convenient, but physically well motivated, procedure for generating a Hopf bifurcation from the trivial state with a nonzero spatial wavenumber and exponentially growing eigenfunctions. In fact, solutions of this type may be expected whenever the linear problem is non-selfadjoint, a situation that we believe to be generic for reaction-diffusion systems of sufficient complexity.

As pointed out by a referee, this remark can be made more explicit within the complex Ginzburg-Landau equation for rotating $m$-armed spirals:

$$A_{rr} + \frac{1}{r}A_r - \frac{m^2}{r^2}A + (1 + i\alpha)A - (1 + i\gamma)A|A|^2 = 0. \tag{17}$$

In this model the coefficient $\alpha$ involves the wave frequency $\omega$, i.e., $\mathrm{d}\alpha/\mathrm{d}\omega \neq 0$. Kopell and Howard [21] show rigorously that when $\gamma$ is small it is possible to choose a nonzero but small $\alpha$ (by varying $\omega$ near zero) such that equation (17) has a spiral-wave solution (see also Hagan [16] and Scheel [30]). In the core ($r \ll 1$) $A$ is small and its radial growth is governed by the *linear* equation

$$A_{rr} + \frac{1}{r}A_r - \frac{m^2}{r^2}A + (1 + i\alpha)A = 0, \tag{18}$$

whose solutions are complex Bessel functions when $\alpha \neq 0$. Thus the matching procedure when $0 < \gamma \ll 1$ selects a nonzero $\alpha$ and hence complex Bessel functions for the core

solution. Since Robin boundary conditions also select complex Bessel functions, it is plausible that there is a meaningful connection between the matching condition used in the above papers and the Robin boundary conditions employed here. Since the latter approach applies to systems undergoing a Hopf bifurcation to oscillations with a finite wavenumber (unlike the complex Ginzburg-Landau equation) the approach of this paper may be viewed as a generalization of existing work on $\lambda - \omega$ systems to such systems and to systems which are far from variational.

We hope that these conclusions will spur additional efforts to study cores of spirals and of target patterns, as done by Müller et al. [24]. Such studies should resolve the structure of the core, which holds the key to the linear stability problem that produces these objects in the first place. It is of interest to note that Steinbock and Müller [32] found that an artificial enlargement of the core (by optical means) results in a substantially increased wavelength of the waves outside the core. We interpret this experiment as lowering the value of $\sigma$ and thus taking the system closer to threshold. The experimental observations are in qualitative agreement with the scenario outlined above. Similar behavior has also been seen in simulations of the Oregonator model as the propagation boundary is approached, Jahnke and Winfree [19].

What about spirals on the infinite plane? The limit $R \to \infty$ is mathematically problematic. Formally, our results suggest that the region in which the weakly nonlinear theory applies shrinks to zero. The instability is then to a mode that grows exponentially in $r$. The solution therefore becomes fully nonlinear immediately at onset with no intermediate weakly nonlinear regime in which the solution resembles the linear eigenfunction over the whole domain. We believe that this observation lies at the root of the difficulty of identifying bifurcations to spirals or target patterns in unbounded domains.

## Acknowledgement

We are grateful to W. Jäger and S. Tobias for numerous discussions, and a referee for helpful comments. This research was supported in part by the National Science Foundation under Grants DMS-9704980 (MG) and DMS-9703684 (EK), and the Texas Advanced Research Program (003652037) (MG).

## References

[1] I. S. Aranson, L. Aranson, L. Kramer, and A. Weber. Stability limits of spirals and traveling waves in nonequilibrium media, *Phys. Rev. A* **46** (1992) R2992–2995.

[2] G. Auchmuty. Bifurcation analysis of reaction-diffusion equations V. Rotating waves on a disk. In *Partial Differential Equations and Dynamical Systems* (W. E. Fitzgibbon III, ed.) Res. Notes Math. **101**, Pitman Press, Boston, 1984, 35–63.

[3] A. Bers. Space-time evolution of plasma instabilities—Absolute and convective. In *Handbook of Plasma Physics* (M. N. Rosenbluth and R. Z. Sagdeev, eds.), vol. 1, North-Holland, Amsterdam, pp. 451–517.

[4] E. Bodenschatz, J. R. de Bruyn, G. Ahlers, and D. S. Cannell. Transition between patterns in thermal convection, *Phys. Rev. Lett.* **67** (1991) 3078–3081.

[5] R. Courant and D. Hilbert. *Methods of Mathematical Physics*. Interscience Publishers, New York, 1953.

[6] M. C. Cross and P. C. Hohenberg. Pattern formation outside of equilibrium, *Rev. Mod. Phys.* **65** (1993) 851–1112.
[7] M. Dellnitz, M. Golubitsky, A. Hohmann, and I. N. Stewart. Spirals in scalar reaction diffusion equations, *Intern. J. Bifur. & Chaos* **5** (1995) 1487–1501.
[8] J. A. DeSimone, D. L. Beil, and L. E. Scriven. Ferroin-collodion membranes: Dynamic concentration patterns in planar membranes, *Science* **180** (1973) 946–948.
[9] M. Eiswirth, M. Bär, and H. H. Rotermund. Spatiotemporal selforganization on isothermal catalysts, *Physica D* **84** (1995) 40–57.
[10] S. Friedlander and W. L. Siegmann, Internal waves in a contained rotating stratified fluid, *J. Fluid Mech.* **114** (1982) 123–156.
[11] H. F. Goldstein, E. Knobloch, I. Mercader, and M. Net. Convection in a rotating cylinder. Part 1. Linear theory for moderate Prandtl numbers, *J. Fluid Mech.* **248** (1993) 583–604.
[12] M. Golubitsky, V. G. LeBlanc, and I. Melbourne. Hopf bifurcation from rotating waves and patterns in physical space, *J. Nonlin. Sci.* To appear.
[13] M. Golubitsky, I. N. Stewart, and D. G. Schaeffer. *Singularities and Groups in Bifurcation Theory*, vol. 2. Applied Mathematical Sciences **69**, Springer-Verlag, New York, 1988.
[14] M. Gorman, M. el-Hamdi, and K. A. Robbins. Experimental observations of ordered states of cellular flames, *Comb. Sci. & Tech.* **98** (1994) 37–45.
[15] J. Greenberg. Axi-symmetric, time-periodic solutions to $\lambda - \omega$ systems, *SIAM J. Appl. Math.* **34** (1978) 391–397.
[16] P. Hagan. Spiral waves in reaction-diffusion equations, *SIAM J. Appl. Math.* **42** (1982) 762–786.
[17] N. Hartmann, M. Bär, I. G. Kevrekidis, K. Krischer, and R. Imbihl. Rotating chemical waves in small circular domains, *Phys. Rev. Lett.* **76** (1996) 1384–1387.
[18] P. Huerre and P. A. Monkewitz. Local and global instabilities in spatially developing flows, *Ann. Rev. Fluid Mech.* **22** (1990) 473–537.
[19] W. Jahnke and A. T. Winfree. A survey of spiral-wave behaviors in the Oregonator model, *Intern. J. Bifur. & Chaos* **1** (1991) 445–466.
[20] S. V. Kiyashko, L. N. Korzinov, M. I. Rabinovich, and L. S. Tsimring. Rotating spirals in a Faraday experiment, *Phys. Rev. E* **54** (1996) 5037–5040.
[21] N. Kopell and L. N. Howard. Target pattern and spiral solutions to reaction-diffusion equations with more than one space dimension, *Advances in Appl. Math.* **2** (1981) 417–449.
[22] L. Kramer, F. Hynne, P. Graae Soerenson, and D. Walgraef. The Ginzburg-Landau approach to oscillatory media, *Chaos* **4** (1994) 443–452.
[23] I. Mercader, M. Net, and E. Knobloch. Binary fluid convection in a cylinder, *Phys. Rev. E* **51** (1995) 339–350.
[24] S. C. Müller, T. Plesser, and B. Hess. The structure of the core of the spiral wave in the Belousov-Zhabotinskii reaction, *Science* **240** (1985) 661–663.
[25] S. C. Müller, T. Plesser, and B. Hess. Two-dimensional spectrophotometry of spiral wave propagation in the Belousov-Zhabotinskii reaction, *Physica D* **24** (1987) 71–86.
[26] J. D. Murray. *Mathematical Biology*. Biomath. **19**, Springer-Verlag, New York, 1989.
[27] P. C. Newell. Attraction and adhesion in the slime mold *Dictyostelium*. In *Fungal Differentiation: A Contemporary Synthesis*, J. E. Smith (ed), Mycology Series **43**, Marcel Dekker, New York (1983) 43–71.
[28] M. Bär and M. Or-Guil. Alternative scenarios of spiral breakup in a reaction-diffusion model with excitable and oscillatory dynamics, *Phys. Rev. Lett.* **82** (1999) 1160–1163.
[29] A. Palacios, G. H. Gunaratne, M. Gorman, and K. A. Robbins. Cellular pattern formation in circular domains, *Chaos* **7** (1997) 463–475.
[30] A. Scheel. Bifurcation to spiral waves in reaction-diffusion systems, *SIAM J. Math. Anal.* **29** (1998) 1399–1418.
[31] A. Scheel. Subcritical bifurcation to infinitely many rotating waves, *J. Math. Anal. Appl.* **215** (1997) 252–261.
[32] O. Steinbock and S. C. Müller. Chemical spiral rotation is controlled by light-induced artificial cores, *Physica A* **188** (1992) 61–67.

[33] S. M. Tobias and E. Knobloch. On the breakup of spiral waves into chemical turbulence, *Phys. Rev. Lett.* **80** (1998) 4811–4814.
[34] S. M. Tobias, M. R. E. Proctor, and E. Knobloch. Convective and absolute instabilities of fluid flows in finite geometry, *Physica D* **113** (1998) 43–72.
[35] P. B. Umbanhowar, F. Melo, and H. L. Swinney. Periodic, aperiodic, and transient patterns in vibrated granular layers, *Physica A* **249** (1998) 1–9.
[36] E. T. Whittaker and G. N. Watson. *A Course of Modern Analysis*. Cambridge U. Press, Cambridge, 1965.
[37] A. T. Winfree. Rotating chemical reactions, *Scientific American*, June 1974, 82–95.
[38] A. T. Winfree (ed.), Focus Issue: Fibrilation in Normal Ventricular Myocardium, *Chaos* **8** (1998).
[39] V. S. Zykov and S. C. Müller. Spiral waves on circular and spherical domains of excitable medium, *Physica D* **97** (1996) 322–332.